In situ study of fiber structure development of poly(butylene terephthalate) in a continuous laser-heated drawing process

Kyoung-Hou Kim[a], Young-Ah Kang[b], Aki Yokoyama[c], Toshifumi Ikaga[c], Yutaka Ohkoshi[c, *], Isao Wataoka[d], Hiroshi Urakawa[d]

[a]*Textile & Consumer Goods Examination Division, Korean Intellectual Property Office, Government Complex Daejeon Building 4, 189, Cheongsa-ro, Seo-gu, Daejeon 302-701, Republic of Korea*

[b]*Research Institute of Human Ecology, Dong-A University, 840 Hadan2-dong, Saha-gu, Busan 604-714, Republic of Korea*

[c]*Faculty of Textile Science and Technology, Shinshu University, 3-15-1 Tokida, Ueda, Nagano 386-8567, Japan*

[d]*Graduate School of Science and Technology, Kyoto Institute of Technology, Goshokaidoucho, Matsugasaki, Sakyo-ku, Kyoto 606-8585, Japan*

ABSTRACT

The structural development of poly(butylene terephthalate) (PBT) fibers was analyzed using *in situ* wide angle X-ray diffraction and fiber temperature measurements during CO_2 laser-heated drawing, in which the necking position on the running fiber could be fixed by CO_2 laser irradiation. The measured parameters were determined as functions of the elapsed time after necking with a time resolution of 0.3 ms. The as-spun PBT fibers, which exhibited a low-oriented α-crystalline structure, were drawn to a draw ratio of 5 using laser heating. The (001') reflection, which indicates a quasi-smectic fibrillar structure, was not observed prior to crystallization in contrast to measurements of poly(ethylene terephthalate) and poly(ethylene 2,6-naphthalene dicarboxylate). The α-crystal was transformed into an oriented β-form crystal at the necking position, and the developed β-crystallites exhibited increased size and altered orientation less than 2 ms after necking. The fiber temperature increased rapidly at around T_g, and the rearrangement of the β-crystal primarily occurred as the fiber's temperature rose from 100°C to 160°C. The oriented β-crystal of the drawn fiber transformed into the oriented α-crystal when the drawing tension was released.

Keywords: poly(butylene terephthalate), laser-heated drawing, crystal-crystal transition

1. Introduction

Poly(butylene terephthalate) (PBT) is a type of polyester produced by the polymerization of 1,4-butanediol and terephthalic acid. PBT has two more methylene (CH_2) groups than poly(ethylene terephthalate) (PET), which results in reduced coherence among molecules and provides the PBT fiber with increased flexibility. The higher chain flexibility causes a reversible crystal-crystal transition, and the PBT

fiber thus exhibits good stretching properties with high stretch recovery.

PBT has two different crystalline forms: the α-form and the β-form [1-7]. The α-form crystalline structure, in which the chain consists of four methylene groups with a *gauche-trans-gauche* conformation, is found in a relaxed state and is the most stable structure. The α-crystal is transformed into the β-crystal when the polymer is held under strain, and the polymer reversibly transforms to the α-crystal upon removal of the strain. The β-crystal consists of an all-*trans* conformation chain. This difference in conformation between the β-crystal and the α-crystal, which is not fully extended, primarily affects the unit cell parameter *c*, which is very sensitive to the transition and is often used to detect the transition. Mencik [1] was the first to index the unit cell of the α-crystal, which is triclinic and has lattice parameters of *a*=0.483 nm, *b*=0.596 nm, *c*=1.162 nm, α=99.9°, β=115.2°, and γ=113.8°. Yokouchi et al. [6] proposed that the α-crystal exhibits ca. 68° internal rotation of the methylene bonds, that the terephthalate segment is nonplanar with the carbonyl bonds, and that the β-phase structure has lattice parameters of *a*=0.473 nm, *b*=0.575 nm, *c*=1.311 nm, α=104.2°, β=120.8°, and γ=100.9°. Hall and Pass [7] claimed that the α-crystal has 77° internal rotation of the methylene bonds and that the terephthalate segment is coplanar with the carbonyls. They also proposed a different β-crystal with dimensions of *a*=0.469 nm, *b*=0.580 nm, *c*=1.300 nm, α=101.9°, β=120.5°, and γ=105.0°. In this work, we report *in situ* wide-angle X-ray diffraction (WAXD) measurements and fiber temperature studies on the reversible crystal structure transition during the fiber structure development of PBT during neck deformation.

Our research group has previously used synchrotron X-ray diffraction measurements to investigate fiber structure development during continuous laser-heated drawing of a running fiber [8-14]. The measured parameters were determined as functions of the elapsed time, which was calculated using the distance between the measurement point and the necking position. This calculation allows good time resolution because the necking is confined to a narrow region in which CO_2 laser radiation produces rapid and uniform heating. We successfully conducted the *in situ* analyses with a temporal resolution of less than 1 ms. This study focused on the elapsed time between the occurrence of necking and the crystal-crystal transition in a PBT fiber during fiber structure development by CO_2 laser-heated drawing.

2. Experimental

2.1. CO₂ laser absorption coefficient

The CO_2 laser absorption coefficient of PBT was evaluated using an infrared spectrometer (Perkin-Elmer FT-IR 1600). The CO_2 laser light used in this study had a wavelength of 10.6 μm, corresponding to an absorbance of 943 cm^{-1}. Infrared absorption spectra were obtained using six PBT films with thicknesses of 50, 60, 91, 150, 170, and 210 mm, and the absorbance was extrapolated based on the film thicknesses. Infrared spectra were obtained using 64 integrations with a resolution of 2 cm^{-1}. Ultimately, the absorption coefficient of PBT was found to be 8.1×10^4 m^{-1}, which is very high in comparison to other polyesters such

as PET, PTT, and PEN [8-11].

2.2. Fundamentals of in situ measurements

The *in situ* measurement system used in this study is schematically illustrated in Figure 1. The details of the *in situ* measurements described here can be found in our previous papers [8-14]. The running fiber was heated using a CO_2 laser beam generated by a PIN-20S laser source (manufactured by Onizuka Co. Ltd). The fiber was irradiated from three directions to minimize its cross-sectional temperature variation. The laser source had a rated power of 20±1 W with a beam diameter of 5 mm. Highly stable neck drawing in which the neck-drawing point fluctuated within approximately 1 mm was possible in this *in situ* analysis because this laser irradiation technique can rapidly and homogeneously heat the running fiber with no contact. The applied laser power was measured using a PW-250 powermeter from SYNRAD Co. Ltd, and the drawing stress was measured using a 100 gf sensor and a HS-1500S tensionmeter from EIKO SOKKI Co. Ltd. The running fiber was drawn by applying a speed differential between the feed and take-up rollers. X-ray diffraction data and the fiber temperature were measured as functions of elapsed time t, which was calculated from the distance X between the measurement and necking points divided by the fiber running speed v. The distance X was controlled by shifting the necking position using a traveling mirror unit, as described in the previous reports [8-14].

2.3. Material

The PBT pellets ([η]=0.85 dl/g) used in this study were melted and extruded through a single-hole spinneret with a 1.0 mm diameter (L/D=5) at 270°C. The throughput rate was set to 3.6 g/min. The spinning line was not equipped with a quenching air apparatus. The fiber was taken up with a speed of 361 m/min, and the as-spun PBT fiber had a diameter of approximately 100 μm.

2.4. Neck drawing and time resolution

The as-spun PBT monofilament was drawn to a draw ratio of 5.0 at a feed speed of 18 m/min and a laser power of 11.0 W. The drawing stress was 0.11 GPa. The neck-drawing point was observed using a TK-C1461 CCD camera from VICTOR Co. equipped a TV-1M telecentric lens from OPTART Co.

The time resolution of each measurement point was estimated by dividing the resolution of the necking point position measurement by the fiber running speed. The resolution of the necking point position (W_{x-ray}) was calculated using Eq. (1) based on the width of the X-ray beam (W_{beam}), the fluctuation of the necking point (W_{neck}), and the length of the necking deformation (W_{deform}). W_{neck}, W_{deform}, and the average necking position were estimated by analyzing the CCD camera images around the necking point. The time resolution was primarily influenced by W_{neck} and W_{beam} and was found to be 0.3 ms.

$$W_{X-ray} = \sqrt{W_{beam}{}^2 + W_{neck}{}^2 + W_{deform}{}^2}$$ (1)

2.5. Wide angle X-ray diffraction measurement

Beam line 40B2 of the synchrotron radiation X-ray source at the SPring-8 facility was used in this study. The X-ray beam diameter (W_{beam}) was 0.2 mm, and the applied wavelength was 0.08 nm. WAXD images were taken using a 3000×3000 pixel imaging plate with a 400-mm-long vacuum chamber and an exposure time of 480 s. The sample-to-detector distance was calibrated using the diffraction patterns of lead dioxide (PbO_2) and hexamethylenetetramine ($C_6H_{12}N_4$). The necking point was located using the X-ray intensity profile transmitted through an ion chamber. The intensity profile of the reflection from a polyimide film mounted on the vacuum chamber was used as a reference profile by subtracting a blank image. Additional details of the *in situ* WAXD measurement can be found in our previous reports [8-14].

The position θ_0 and the half width σ were determined by fitting the measurements to a Gaussian function (2). The effect of beam divergence on σ was corrected using the width of the PbO_2 intensity profiles. The *d*-spacing and crystallite size D were calculated using Bragg's equation (3) and Scherer's equation (4), respectively, with a constant k of 0.918. The crystal orientation factor f was estimated by fitting the azimuthal intensity profiles of equatorial (010), (100), and (-104) reflections to the Pearson VII function (Eq. (5)) and then using the fitted profiles in Eq. (6) .

$$I(\phi) = I_0 \exp\left\{ -4\ln 2 \cdot \left(\frac{\theta - \theta_0}{\sigma} \right)^2 \right\}$$ (2)

$$2d \sin \theta_0 = \lambda$$ (3)

$$D = \frac{k\lambda}{\sigma \cos \theta_0}$$ (4)

$$I(\beta) = -\frac{I_0}{\left\{ 1 + 4\left(\frac{\beta - \beta_0}{\tau} \right)^2 \left(2^{\frac{1}{2.5}} - 1 \right) \right\}^{2.5}}$$ (5)

$$f = \frac{3\langle \cos^2 \beta \rangle - 1}{2}, \quad \langle \cos^2 \beta \rangle = \frac{\int_0^{\pi/2} I(\beta) \cos^2 \beta \sin \beta d\beta}{\int_0^{\pi/2} I(\beta) \sin \beta d\beta}$$ (6)

2.6. Fiber temperature measurement

The fiber temperature was measured using an infrared thermo-spot sensor (TNZ7N2-J0-5K1-2 type, Japan Sensor Co., Ltd) equipped with a HgCdTe sensor and an interference filter. The response time of this sensor was 10 ms. The interference filter transmits a wavelength of 5.78±0.1 μm, which corresponds to the absorbance band due to C=O stretching. The *in situ* fiber temperature measurement was conducted in the

same manner as in the previous studies [8-14].

3. Results and Discussion

3.1. Fiber temperature

To determine the change in fiber temperature during the laser-heated drawing, the fiber temperature profile as a function of distance from the necking point was obtained and is presented in Figure 2. The origin of the horizontal axis in Figure 2 designates the necking point, and the shaded region denotes the region irradiated by the laser beam. The fiber temperature was measured twice under each set of conditions to confirm the reproducibility of the measurement, and both results are presented in the figure. The fiber temperatures begin to increase upon entering the laser irradiation region, and increase rapidly from approximately 50°C to 100°C at the necking point, indicating the release of the exothermic heat of plastic deformation instantly followed by necking. The fiber temperatures continue to increase to approximately 160°C at approximately 2 mm, corresponding to 1.3 ms after necking, and then decrease gradually after leaving the laser irradiation region. The temperature change exhibited by PBT is almost the same as that of PET [8, 9, 14] and higher than that of PTT [10]. Because the temperature increase is determined by the drawing stress and the draw ratio [15], it depends on the drawing conditions. It is worth noting that the temperature just after necking, during which the fiber structure is formed, is 120°C to 140°C for PET [8, 9, 14], 110°C to 120°C for PTT [10], and approximately 100°C for PBT. This variation is related to the chain mobility and resultant T_g of each polymer, which are approximately 80°C, 45°C, and 30°C, respectively.

3.2. WAXD analysis

Figure 3 shows WAXD patterns taken at various elapsed times, and the corresponding diffraction intensity profiles in the equatorial and meridian directions are shown in Figures 4(a) and (b). WAXD images at negative elapsed time, representing images of the undrawn fiber, exhibit diffuse equatorial arcs that are superposed on an amorphous halo and the low-oriented α-crystal (010) and (100) reflections near 2θ=8.92° and 11.97°, respectively. At the necking point, the halo and the diffractions are concentrated at the equator, indicating that the molecular chains are oriented along the fiber axis. After necking, the (100) reflection moves to higher 2θ and the equatorial intensities increase as the elapsed time increases. Additionally, a meridian streak representing the β (-104) reflection appears near 2θ=14° at 0.25 ms, and remains stable with elapsed time throughout the drawing process. The drawing stress of 0.11 GPa is sufficient to enable the α to β crystal transition according to a previous study [19]. In the drawn fiber, the meridian streak moves to approximately 2θ=16°, which corresponds to the β to α crystal transition. Because the (-104) plane is almost perpendicular to the *c*-axis, the (-104) interplanar spacing reveals the conformational change from all-*trans* to *gauche-trans-gauche* during the crystal-crystal transition.

Song [16] proposed that a mesophase structure forms when amorphous PBT is stretched at room temperature, and Konishi and Miyamoto [17] suggested that a mesophase structure on the nanometer scale forms when PBT crystallizes from the glassy state. This mesophase, which has a quasi-smectic fibrillar structure as revealed by the (001') reflection, transformed into the α-form. The smectic periodicity was 1.169 nm, which corresponds to the c-axis length of the α-crystalline unit cell [16]. A similar smectic structure was observed in our previous studies on PET and poly(ethylene 2,6-naphthalene dicarboxylate) (PEN) [8, 9, 11, 14] and was formed just after necking and prior to crystallization. However, in this study, no obvious quasi-smectic fibrillar structure was observed during the laser-heated drawing of PBT, likely because the transformation from the PBT mesophase to the crystalline structure occurs too rapidly to be observed with this measurement's time resolution of 0.3 ms.

3.3. Interplanar spacings

Figures 5(a)-(c) present the changes in the *d*-spacings of the (010), (100), and (-104) reflections, respectively, versus elapsed time. The (100) *d*-spacing increased slightly in the 2 ms following necking and then decreased as the elapsed time increased beyond 2 ms. The (-104) and (010) *d*-spacings of the drawn fiber decreased with respect to the values observed during drawing, and the (100) *d*-spacing increased. Although all the measured *d*-spacings were larger than the calculated values for the reported unit cells [1, 6, 7], it is reasonable to conclude that the samples are in the β-crystal orientation, except for the "drawn" sample. The differences should be caused by molecular packing in the equatorial directions but can also be caused by the applied stress in the meridional direction. The initial increase in the *d*-spacings within 2 ms following necking may be caused by thermal expansion, as the fiber temperature reaches a maximum of approximately 160°C at 1.3 ms after necking. After 2 ms, the decrease in the (100) *d*-spacing of the β-crystal with increasing elapsed time may be attributed to both thermal shrinkage and refinement of the molecular packing as the internal rotation angle of the flexible methylene segments changes. This result may imply that the terephthalate segments were arranged closely and parallel to each other. The gentle increase in the (-104) *d*-spacing with elapsed time beyond 2 ms after necking may indicate that the molecular chains extend slightly in the all-*trans* conformation. Ultimately, the large decrease in the (-104) *d*-spacing in the drawn fiber should be caused by the crystal-crystal transition from the β- to the α-crystal form when the drawing tension is released.

3.2. Crystallite sizes and crystallization rate

Figure 6 presents the changes in crystallite sizes of the (010), (100), and (-104) planes, determined using Scherer's equation (Eq. (4)), versus elapsed time. The crystallite sizes of the (010), (100), and (-104) planes increased sharply up to 2 ms after necking and then remained nearly unchanged with further elapsed time. This indicates that β-phase crystallites were formed and increased in size within 2 ms after the crystal-

crystal transition and then stopped growing, which seems to occur because the fiber temperature reaches a maximum at 1.3 ms after necking.

Figure 7 presents the crystallinity indices ($X(t)$) estimated from the integrated intensities of the equatorial reflections. By fitting these intensities to an Avrami-type equation (Eq. (7)), a crystallization rate (K_c) of approximately 400 s^{-1} was determined. Although this is lower than the crystallization rates of other polyester fibers investigated in our previous studies [8-11,14], it does not indicate slower orientation-induced crystallization of PBT because no X_0 was assumed in the previous studies. Because no mesophase structure was observed in this study, the primary orientation-induced crystallization from the low-oriented α-crystal to the high-oriented β-crystal is considered to be completed within 0.25 ms of necking, and the increase in crystallinity presented in Figure 7 can be considered to be attributed to secondary crystallization. The primary crystallization of PBT occurs much more rapidly than that of PET, which could be caused by the difference in the as-spun fiber; the as-spun PBT fiber used in this study was already crystallized to some extent because of the low T_g, while the PET, PTT, and PEN fibers used in previous studies were nearly amorphous before drawing. *In situ* measurements with shorter time resolutions are needed for further discussion of this issue.

$$\frac{X(t) - X_0}{X_\infty - X_0} = 1 - \exp(-K_c t) \tag{7}$$

3.3. Crystal orientation

Figure 8 shows the crystal orientation factors of the (010), (100), and (-104) planes versus elapsed time. The crystal orientation factors of the (010) and (-104) planes increased rapidly during the first 2 ms after necking and then leveled off as the elapsed time increased. The crystal orientation factor of the (100) plane also increased steeply during the first 2 ms but then slowly decreased by approximately 0.5% as the elapsed time increased. Similar to the observed crystallite sizes, this result indicates that the crystal orientations increased as the fiber temperature increased through rearrangement of the β-crystal. In the drawn fiber, the α-crystal form observed after drawing is well-oriented, and the crystallinity index or crystal orientation did not decrease compared to the β-crystallinity index and orientation observed during drawing.

4. Conclusion

The structural development of PBT fibers was analyzed using *in situ* X-ray diffraction and fiber temperature measurements with a time resolution of 0.3 ms. The as-spun PBT fiber, which was low-oriented α-crystalline, was drawn to a draw ratio of 5 through laser heating. The fiber temperature sharply increased from 50°C to 100°C at the necking point. An oriented β-crystal was formed just after necking, but no quasi-smectic fibrillar structure was observed prior to crystallization. Less than 2 ms after necking, the fiber

temperature increased from 100°C to 160°C, and the crystallite size, orientation, and *d*-spacing (in particular that of the *a*-axis direction) of the β-crystal increased as the elapsed time increased. After 2 ms, the *d*-spacing of the *a*-axis direction decreased as the elapsed time increased. In the drawn fiber, the oriented β-crystal transformed back into the oriented α-phase crystal when the drawing tension was released.

Acknowledgments

References

[1] Mencik, Z., The crystal structure of poly(tetramethylene terephthalate), *J. Polym. Sci. Polym. Phys. Ed.*, **13**, 2173-2181 (1975).

[2] Brereton, M.G., Davis, G.R., Jakeways, R., Smith. T., Ward, I. M., Hysteresis of the stress-induced crystalline phase transition in poly(butylene terephthalate), *Polymer,* **19**, 17-26 (1977).

[3] Tashiro, K., Nakai, Y., Kogayashi, M., Tadokoro, H. Solid-State Transition of Poly(butylene terephthalate) Induced by Mechanical Deformation, *Macromolecules,* **13**, 137-145 (1980).

[4] Roebuck, J., Jakeways, R., Ward, I. M., The existence of a stable β form in oriented poly(butylene terephthalate), *Polymer*, **33**, 227-232 (1992).

[5] Desborough, I. J., Hall, I. H., A comparison of published crystalline structures of poly(tetramethylene terephthalate), *Polymer*, **18**, 825-830 (1977).

[6] Yokouchi, M., Sakakibara, Y., Chatani, Y., Tadokoro, H., Tanaka, T., Yoda, K., Structures of Two Crystalline Forms of Poly(butylene terephthalate) and Reversible Transition between Them by Mechanical Deformation, *Macromolecules*, **9**, 266-273 (1976).

[7] Hall, I. H., Pass, M.G., Chain conformation of poly(tetramethylene terephthalate) and its change with strain, *Polymer,* **17**, 807-816 (1975).

[8] Yamaguchi, T., Kim, K.H., Murata, T., Koide, M., Hitoosa, S., Urakawa, H., Ohkoshi, Y., Gotoh, Y., Nagura, M., Kodera, M., Kajiwara, K., Initial Stage of Fiber Structure Development in the Continuous Drawing of Poly(ethylene terephthalate), *J. Polym. Sci., Part B, Polym. Phys.*, **46**, 2126-2142 (2008).

[9] Kim, K. H., Yamaguchi, T., Ohkoshi, Y., Gotoh, Y., Nagura, M., Urakawa, H., Kodera, M., Kikutani, T., Molecular Weight Dependence of Fiber Structure Development in the Laser Drawing of Poly(ethylene terephthalate) Fibers, *J. Polym. Sci., Part B, Polym. Phys.* **47**, 1653-1665 (2009).

[10] Kim, K. H., Kang, Y. A., Murata, T., Ikehata, S., Ohkoshi, Y., Gotoh. Y., Nagura, M., Koide, M., Urakawa, H., Kotera, M., Initial structure development in the CO_2 laser heated drawing of poly(trimethylene terephthalate) fiber, *Polymer*, **49**, 5705-5713 (2008).

[11] Kim, K. H., Aida, R., Kang, Y. A., Ohkoshi, Y., Gotoh, Y., Nagura, M., Urakawa, H., Mesophase structure discovered through in-situ X-ray measurement in drawing process of poly(ethylene 2,6-naphthalene dicarboxylate) fiber, *Polymer,* **50**, 4429-4431 (2009).

[12] Kang, Y. A., Kim, K. H., Ikehata, S., Ohkoshi, Y., Gotoh, Y., Nagura, M., Koide, M., Urakawa, H., Development of a fiber structure in poly(vinylidene fluoride) by a CO_2 laser-heated drawing process, *Polym. J.*, **42**, 657-662 (2010).

[13] Kang, Y. A., Kim, K. H., Ikehata, S., Ohkoshi, Y., Gotoh, Y., Nagura, M., Urakawa, H., In-situ analysis of fiber structure development for isotactic polypropylene, *Polymer*, **52**, 2044-2050 (2011).

[14] Kim, K. H., Murata, T., Kang, Y. A., Ohkoshi, Y., Gotoh, Y., Nagura, M., Urakawa, H., Microsecond Analysis of Quasi-Smectic Fibrillar Structure in the Continuous Fiber Drawing of Poly(ethylene terephthalate), *Macromolecules*, **44**, 7378–7384 (2011).

[15] Okumura, W., Yamaguchi, T., Ohkoshi, Y., Gotoh, Y. & Nagura, M., Direct measurement of fiber temperature in the continuous drawing process of PET fiber heated by CO_2 laser radiation., *Int. Polym. Proc.* **17**, 124–132 (2002).

[16] Song, K., Formation of polymorphic structure and its influences on properties in uniaxially stretched polybutylene terephthalate films, *J. Appl. Polym. Sci.* **78**, 412-423 (2000).

[17] Konishi, T., Miyamoto, Y., Crystallization of Poly(butylene terephthalate) from the Glass, *Macromolecules*, **43**, 375-383 (2010).

[18] Perry, B. C., Koenig, J. L., Lando, J. B., Relaxation behavior of the beta phase of poly(butylene terephthalate), *Macromolecules*, **20**, 422-427 (1987).

[19] Ward, I. M., Wilding, M. A., The mechanical properties and structure of poly(m-methylene terephthalate) fibers, *J. Polym. Sci., Polym. Phys. Ed.*, **14**, 263-274 (1976).

Figure Captions

Figure 1.   Schematic diagram of the *in situ* measurement system.

Figure 2.   Fiber temperature profile, which was measured twice under each set of conditions. The fiber speed profile is also shown.

Figure 3.   WAXD patterns taken at various elapsed times after necking.

Figure 4.   WAXD intensity profiles along the equator (a) and the meridian (b).

Figure 5.   Interplanar spacings of (010) (a), (100) (b), and (-104) (c) planes. The calculated *d*-spacings of the reported unit cells [1, 6, 7] are also shown.

Figure 6.   Crystallite sizes along the (010), (100), and (-104) planes.

Figure 7.   Crystallinity indices estimated from the equatorial intensity profiles.

Figure 8.   Estimated crystal orientation factors of the (010), (100), and (-104) reflections.
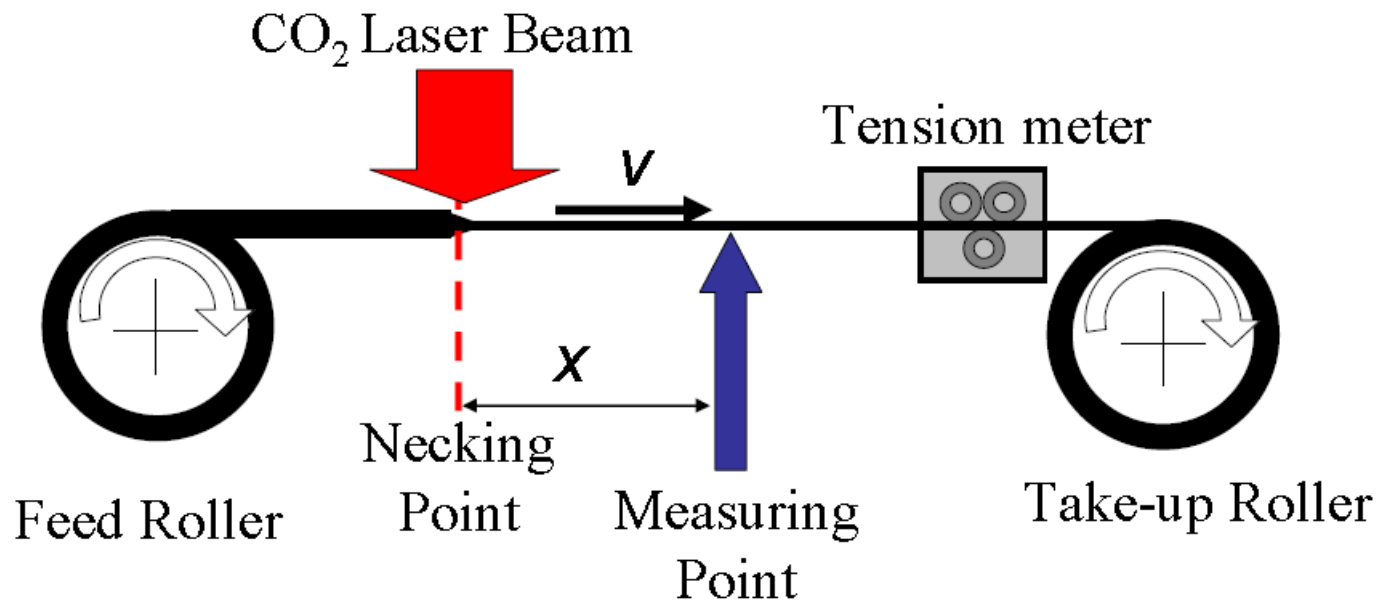
Fig. 1 Schematic diagram of *in-situ* measurement system.
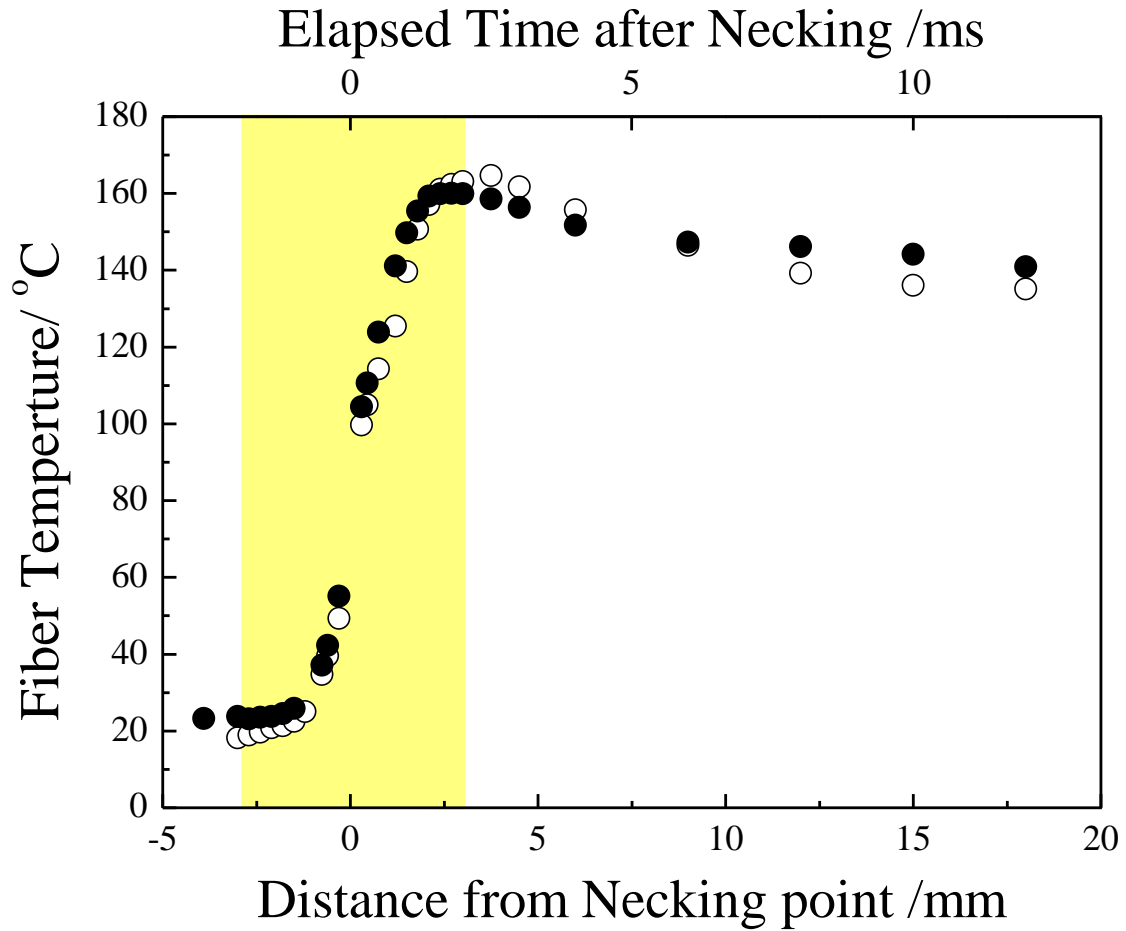
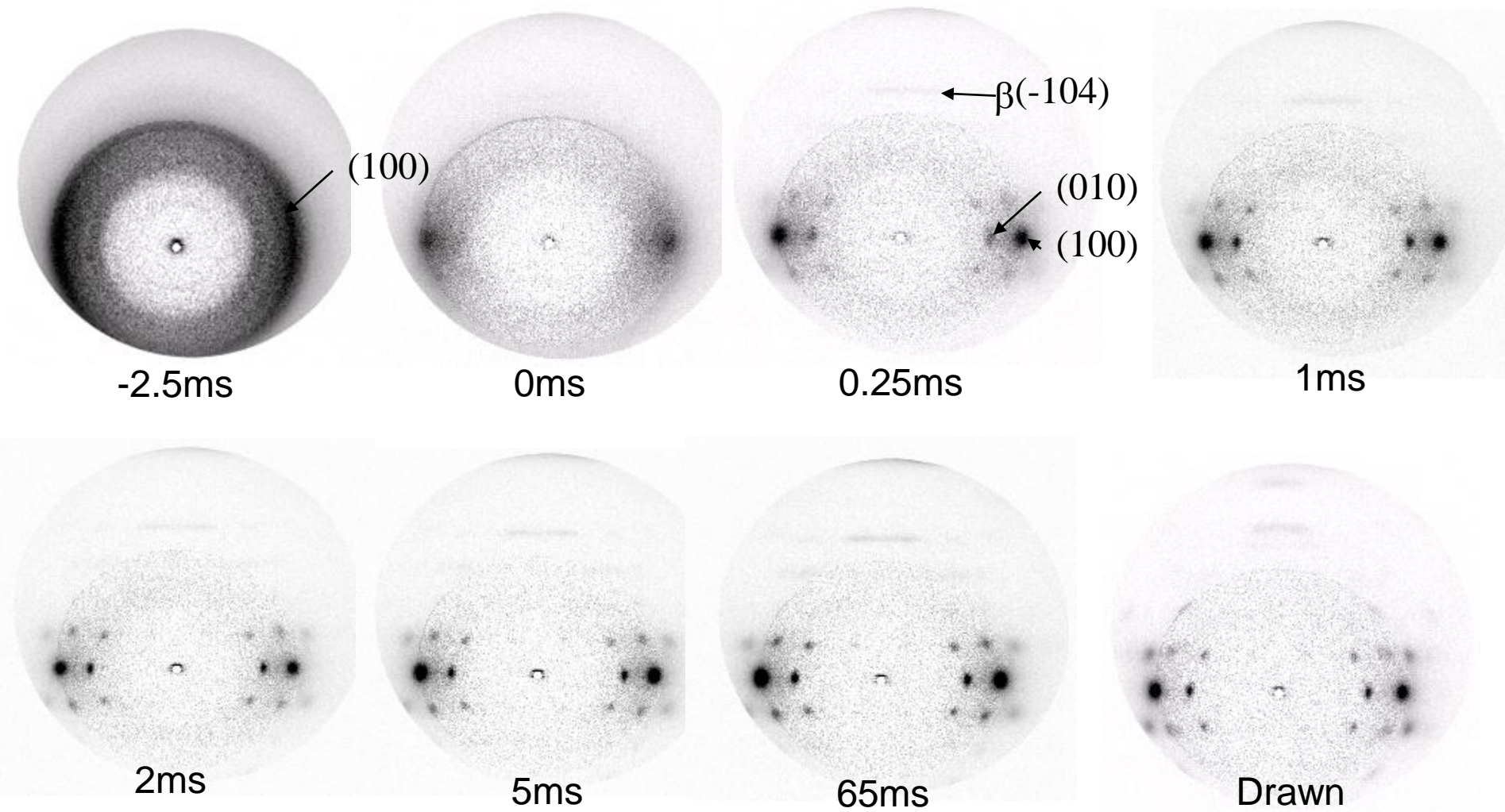Fig. 2 Fiber temperature profile, which was measured twice for each condition.

Fig. 3 WAXD patterns taken at various elapsed times after necking.
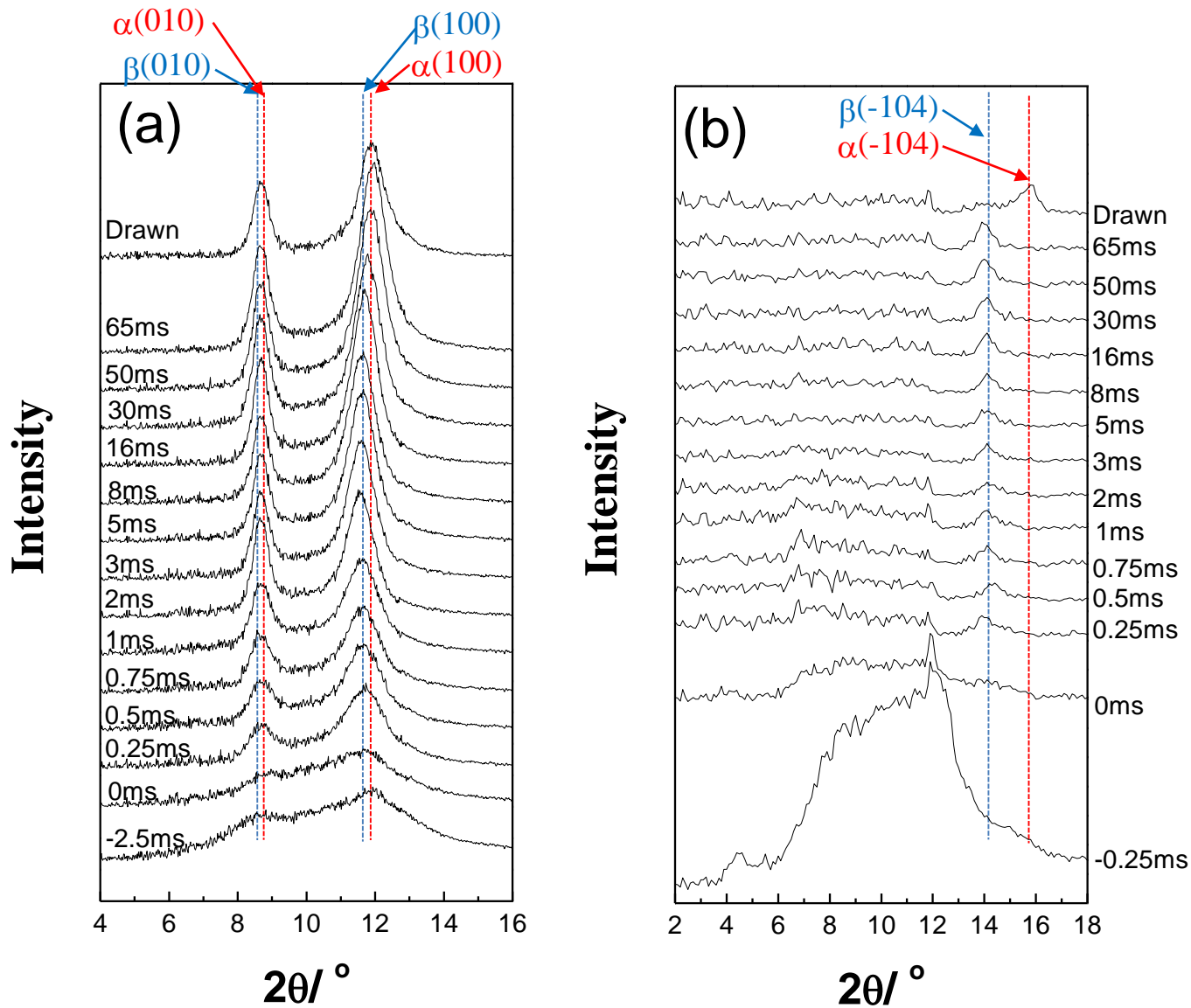
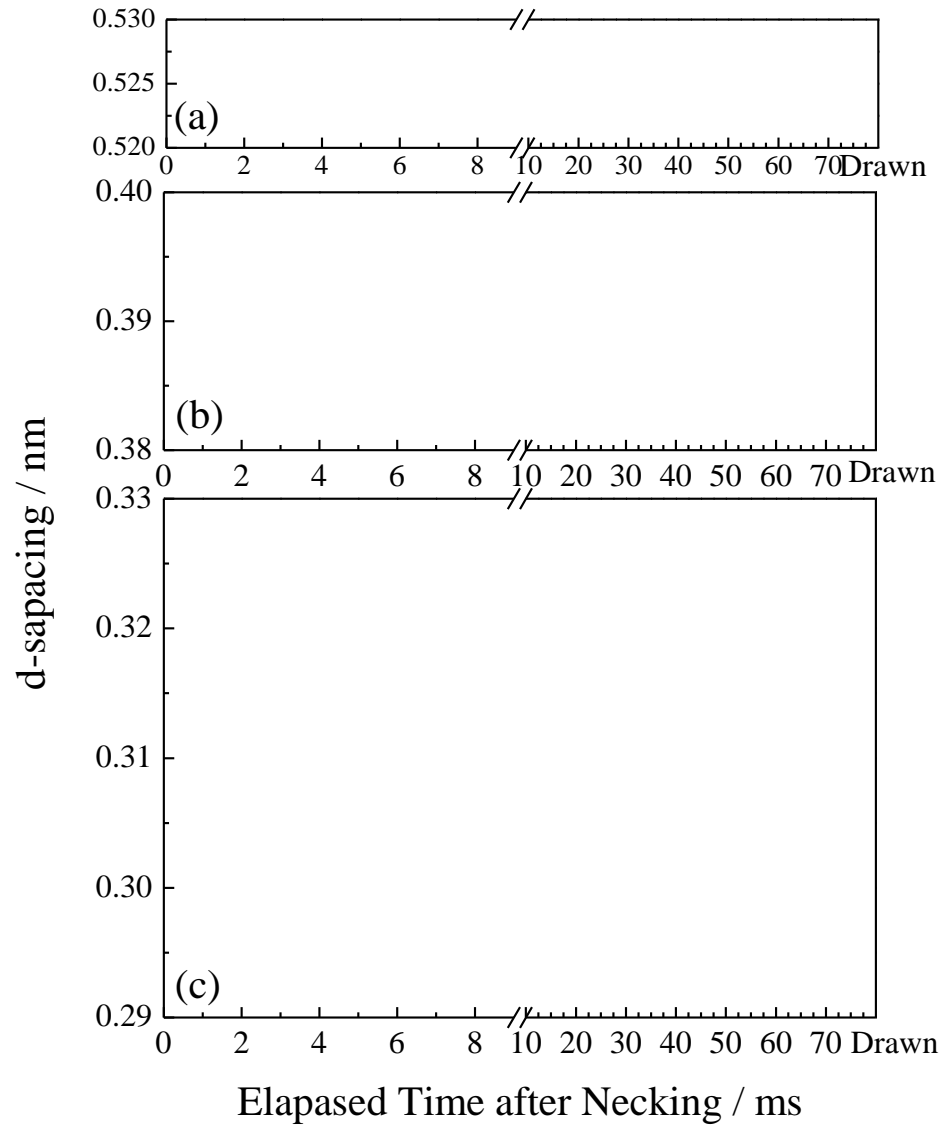Fig. 4 WAXD intensity profiles in equator (a) and meridian (b).

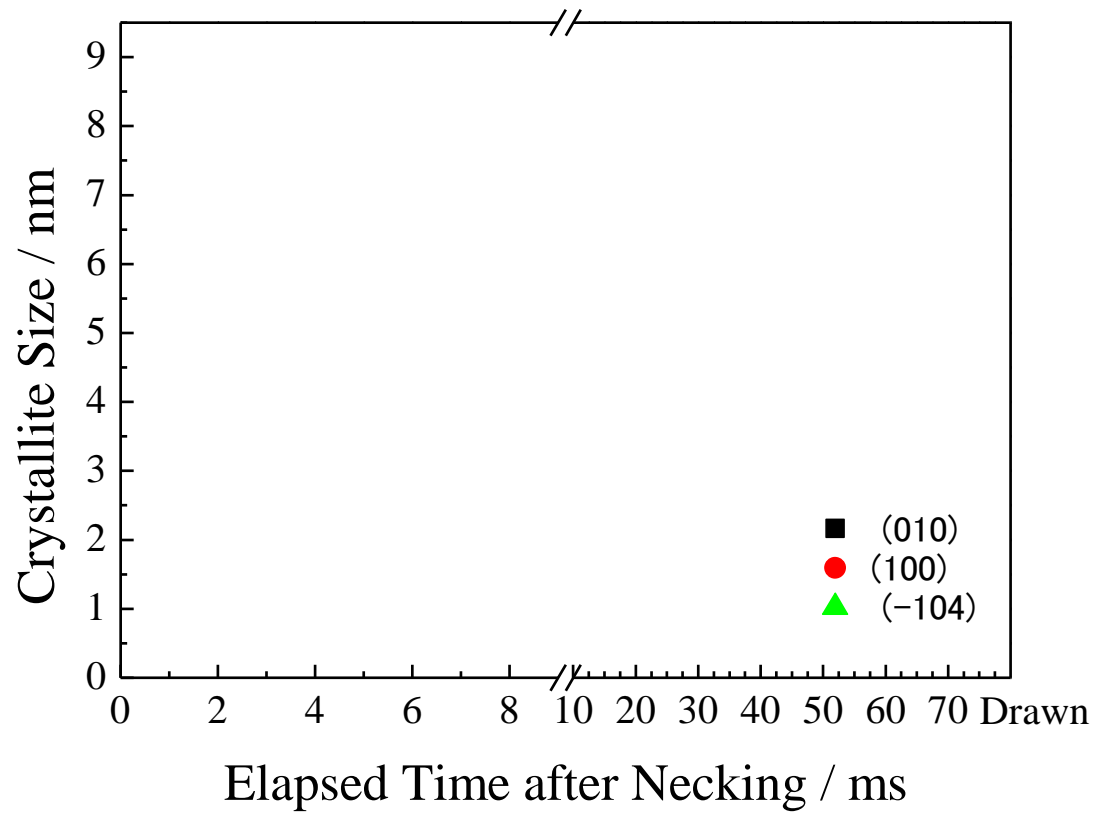Fig. 5 Interplanar spacings of (010) (a), (100) (b), and (-104) (c) planes.

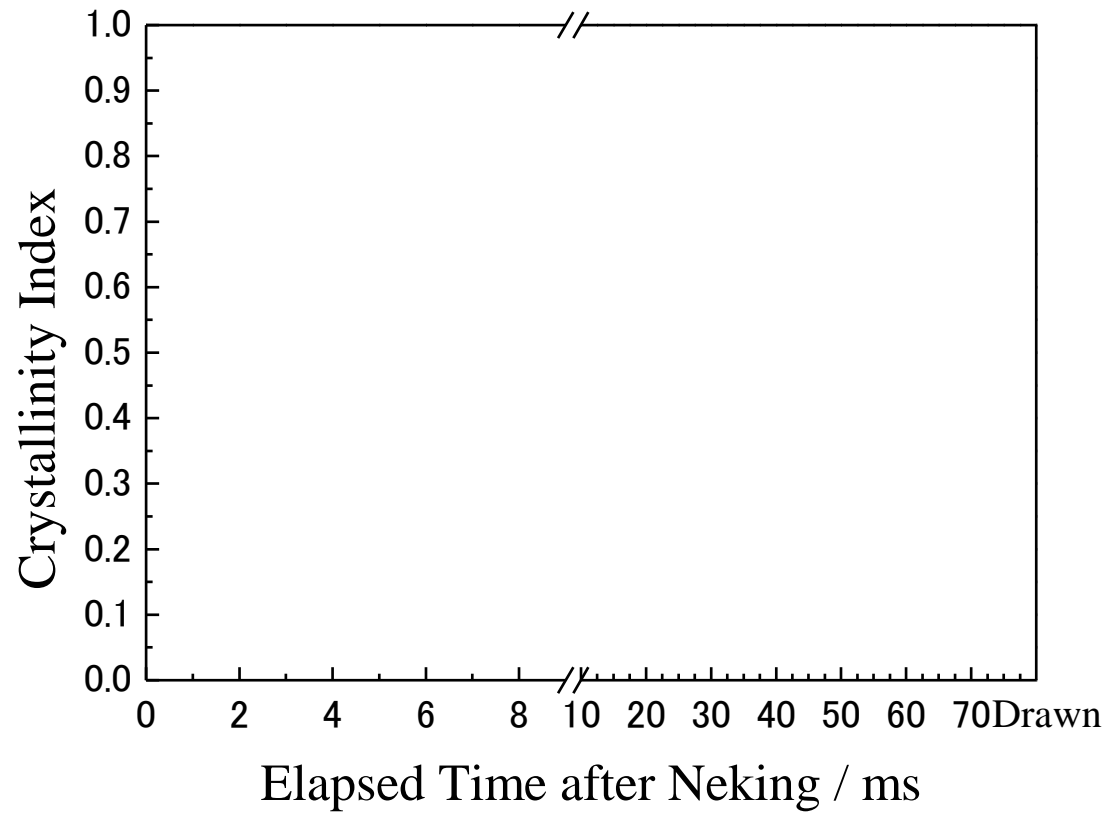Fig. 6 Crystallite sizes along the (010), (100), and (-104) planes.

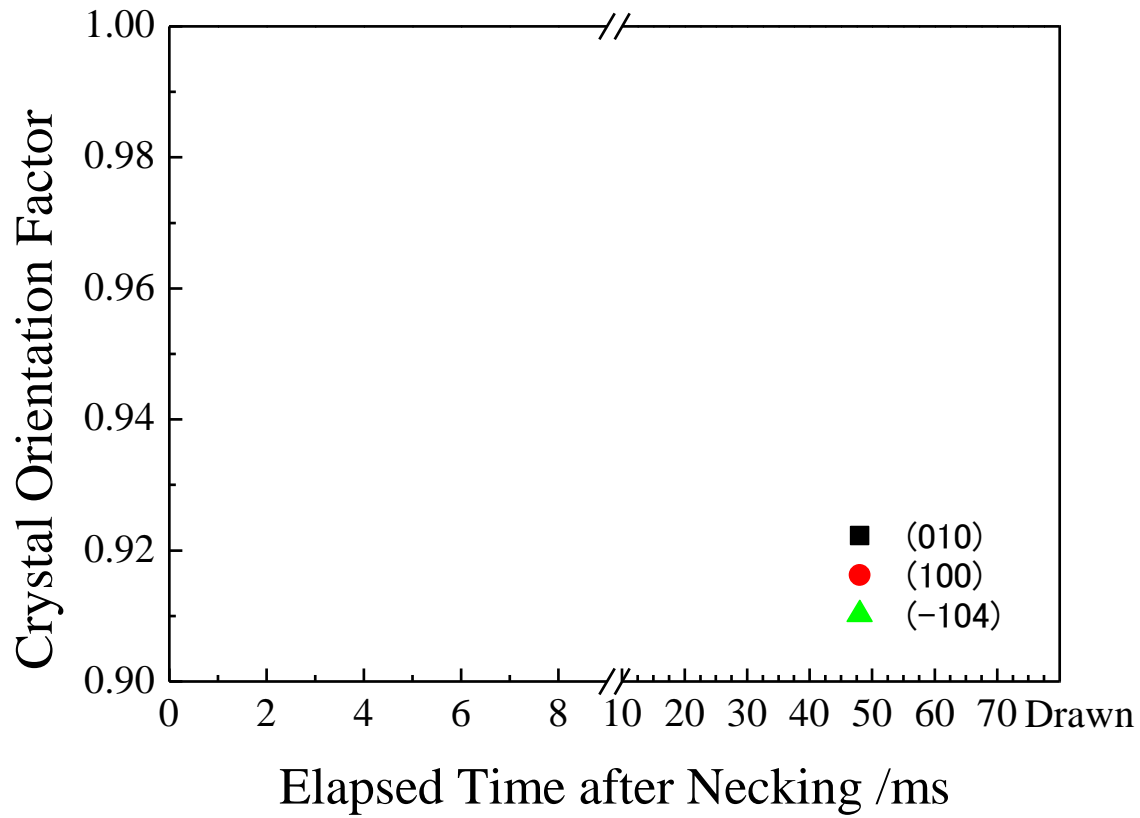Fig. 7 Crystallinity index estimated from the equatorial intensity profiles.

Fig. 8 Crystal orientation factor estimated for (010), (100), and (-104) reflections.